BMC Biotechnology

RESEARCH

Open Access

Enhanced extracellular production of *Coprinopsis cinerea* laccase Lcc9 in *Aspergillus niger* by gene expression cassette and bioprocess optimization

Dongbang Yao[1,2,3], Xiaozhuang Liu[1,2,3], Hui Wang[1,2,3], Juanjuan Liu[1,2,3], Zemin Fang[1,2,3*] and Yazhong Xiao[1,2,3*]

Abstract

Background The laccase Lcc9 from *Coprinopsis cinerea* has optimal catalytic activity at moderate to alkaline pH conditions, making it invaluable for industrial applications. However, *C. cinerea* naturally secretes Lcc9 at low expression levels, which limits the industrial application of Lcc9 on a large scale. Recombinant production of Lcc9 using *Aspergillus niger* would be an effective way to achieve its high production.

Results This study achieved the secretory production of Lcc9 in *A. niger* and established an efficient transformation procedure for *A. niger* by optimizing its protoplast preparation system. The transformation efficiency of *A. niger* was increased 3.8-fold under the optimal system (cell wall digestion enzyme solution: 2% cellulase, 1% snailase, 1% lyticase, and 0.5% lysozyme; incubation time: 3 h; incubation temperature: 37 ℃; culture time: 48 h). The extracellular yield of Lcc9 was enhanced by optimizing gene expression cassette and bioprocess. First, the strain AnGgcL (containing P_{gpdA}) mediated by the SP_{CAT}, a signal peptide of the extracellular high abundance protein catalase, had an extracellular laccase activity of 10 U/L after shake flask fermentation. Then, by optimizing promoter and signal peptide combinations that regulate *lcc9* expression, the strain AnGcgL mediated by P_{citA}-SP_{GlaA} had an extracellular laccase activity of 20 U/L. Subsequently, the strain AnRcgL1 (containing P_{citA}-SP_{GlaA}) obtained by random integration had an extracellular laccase activity of 86 U/L. Sequencing revealed that the *lcc9* expression cassette was integrated into the citrate synthase gene locus in the AnRcgL1 genome in a 9-copy form. By optimizing the microparticle, osmolyte, and Cu^{2+} in the fermentation medium, the AnRcgL1 extracellular laccase activity was further increased to 1566.7 U/L, which was 156.7-fold higher than that of AnGgcL. Furthermore, its extracellular laccase activity was increased to 1961 U/L in a 1-L fermenter.

Conclusions To our knowledge, this study is the first to report the recombinant extracellular production of the *C. cinerea* laccase Lcc9 in *A. niger* and to use SP_{CAT} in the *A. niger* expression system. The results of this study will help accelerate the industrial application of Lcc9. Moreover, the strategy used in this work provides methodological guidance for increasing other exogenous protein yields in *A. niger*.

Keywords Laccase, *Aspergillus niger*, Signal peptide, Promoter, Integration loci, Bioprocess

*Correspondence:
Zemin Fang
zemin_fang@ahu.edu.cn
Yazhong Xiao
yzxiao@ahu.edu.cn
Full list of author information is available at the end of the article

Background

Laccase (EC 1.10.3.2) is a multi-copper oxidase regarded as a green catalyst for its ability to oxidize carboxylic acids, phenols aromatic amine compounds, etc. with water as the only by-product [1]. Laccase has a wide range of natural sources, among which the white rot fungal laccase has a greater application potential than laccases from other sources due to its high redox potential and specific activity [2]. However, the poor stability of fungal laccase in pH-neutral and alkaline environments, as well as low natural secretion yields, severely limit its application in bioethanol production, paper biobleaching, and wastewater treatment [3]. Therefore, it is important to screen alkaline active laccase and realize its efficient production.

Heterologous expression is an effective strategy to increase target protein yields. Many microbial expression systems have been developed for large-scale production of industrial enzymes. Among them, the *Aspergillus niger* expression system, due to its excellent protein secretion ability and inexpensive culture raw material, has been widely used for the recombinant production of target proteins derived from filamentous fungi [4]. However, compared to prokaryotic and eukaryotic chassis hosts such as *Escherichia coli* and *Pichia pastoris*, the low efficiency of genetic transformation in *A. niger* is one of the bottlenecks hindering its development into an efficient protein expression host [5].

To this end, for the polyethylene glycol (PEG)-mediated transformation (PMT) method commonly used in *A. niger*, previous studies have often improved the transformation efficiency by optimizing the protoplast preparation system [4]. For example, by optimizing cell wall digestion enzymes and media components during protoplast preparation of *A. niger* ATCC 20611, the concentration of protoplasts could be increased 11.1-fold, ultimately resulting in approximately 100 resistant transformants per μg of DNA [6].

Although xylanase and lipase, among others, have achieved high expression in *A. niger*, with extracellular expression as high as 28.91 g/L [4], it is noted that the recombinant expression levels of target proteins from various sources in *A. niger* showed significant discrepancy, with the lowest less than 1 mg/L [7]. To increase the recombinant expression level of heterologous proteins in *A. niger*, commonly used strategies include screening and modification of hosts, optimization of gene expression cassette and bioprocess [7, 8].

Promoters and signal peptides (SPs) are two important expression regulatory elements that affect the transcription and secretion of target genes, and are often used as breakthroughs to increase the expression level of target proteins [4]. For example, the extracellular recombinant activity of α-galactosidase in *A. niger* could be increased more than 22-fold to 215.7 U/mL by replacing its natural signal peptide with the SP_{GlaA} [9]. The glyceraldehyde-3-phosphate dehydrogenase promoter (P_{gpdA}) from *Aspergillus nidulans* is a commonly used constitutive promoter in the *A. niger* expression system due to its high transcriptional activity [10], whereas the P_{mbfA} from *A. niger* ATCC 1015 mediated a β-glucuronidase activity that was approximately 2-fold higher than that mediated by P_{gpdA} [11]. Apart from constitutive promoters, inducible promoters also show good performance in mediating exogenous proteins for recombinant expression in *A. niger* [12]. For example, at 20% (w/v) sucrose concentration, the P_{fopA} successfully achieved 7.68-fold higher EGFP expression in *A. niger* ATCC 20611 than that mediated by the constitutive promoter P_{gpdA} [12].

For genomic integration expression, the integration loci of the target gene in the chassis host genome is also an important factor affecting the target protein expression level. Due to unanticipated pleiotropic effects resulting from the disruption of genome-specific loci by target gene integration, certain chromosomal locations are more favorable for recombinant expression of target genes than others [13]. A commonly used integration locus in the *A. niger* expression system is the *glaA* locus, where many target genes have achieved effective recombinant expression, such as nuclease [14] and protease [15]. However, among the 14,165 open reading frames predicted in the *A. niger* genome, only 2% have been experimentally validated [13]. Such a high number of unknowns severely limits the rational screening of potential high-expression integration locus in *A.niger*. Therefore, to achieve high expression of target proteins, target gene expression cassettes are also often integrated into the chassis host genome in a random integration mode [10].

It is well known that the culture environment of recombinant strains significantly affects their production characteristics as well as the structural stability of target proteins [4]. Previous studies have shown that the recombinant expression level of target proteins can be increased by adding microparticles to modulate the filamentous fungal mycelial morphology [16]. For example, the addition of 5 g/L talc increased pectinase activity in *Aspergillus oryzae* by 20% to 26.6 U/mL [17]. In addition, osmolytes can increase soluble natural conformation formation of target proteins and promote their folding by altering the solvent properties of the culture solution [18]. Based on this, Liu et al. increased the recombinant laccase activity in *A. niger* by 372% to 2037.2 U/L by adding 0.5 mol/L proline [19]. In addition, Cu^{2+} can affect the laccase activity by regulating laccase gene transcription or protein structure [20]. A previous report

indicated that the addition of 1 mM Cu^{2+} to the reaction solution could increase the laccase activity of *Streptomyces griseorubens* JSD-1 by 28% [21].

In our previous study, we found that co-culture of *Coprinopsis cinerea* with *Gongronella* sp. w5 could produce laccase Lcc9 with excellent tolerance in moderate to alkaline pH, which could effectively promote the conversion of indigo and thus have great potential for application in the textile dyeing industry [22]. To accelerate the industrial application process of Lcc9, this study utilized *A. niger* for efficient recombinant expression of Lcc9. Therefore, we first recombinantly expressed the *lcc9* cDNA in *A. niger* and optimized its protoplast transformation efficiency. Then, the signal peptide and promoter in the *lcc9* expression cassette as well as its genomic integration loci were sequentially optimized. Finally, the extracellular laccase activity was further enhanced by optimizing the culture environment of the recombinant strain obtained. The logical schematic of this study is shown in Fig. 1.

Materials and methods

Strains, plasmids, and media

The strains and plasmids used in this study are listed in Table 1. *E. coli* JM109 and *A. niger* MA70.15 [23] were used as host strains for plasmid propagation and expression, respectively. The pC3 plasmid information is detailed in Kangdi Hu et al. [23]. Yeast extract peptone dextrose (YPD) medium (2% peptone, 2% glucose, and 1% yeast extract) was used to culture *A. niger* to collect mycelium for protoplast preparation. The high osmolarity czapek agar medium (34% sucrose, 0.3% $NaNO_3$, 0.05% KCl, 0.05% $MgSO_4{\cdot}7H_2O$, 0.001% $FeSO_4{\cdot}7H_2O$, and 1% agar) was used to regenerate protoplasts. Czapex dox (CD) medium (0.3% $NaNO_3$, 0.2% KCl, 0.1% KH_2PO_4, 0.05% $MgSO_4{\cdot}7H_2O$, 2% glucose, 0.001% $FeSO_4{\cdot}7H_2O$ and 0.1 mM $CuSO_4$) supplemented with 0.5 mM 2,2-azino-bis (3-ethylbenzothiazoline-6-sulphonic acid) (ABTS) was to screen for *A. niger* positive transformants. Potato dextrose agar (PDA) plates were used to culture strains for conidia production. The fermentation medium contained 70 mM $NaNO_3$, 7 mM KCl, 200 mM K_2HPO_4, 2 mM $MgSO_4$, 2% (w/v) glucose, and 1‰ (v/v) trace elements. The trace element content is 76 mM $ZnSO_4$, 25 mM $MnCl_2$, 18 mM $FeSO_4$, 7.1 mM $CoCl_2$, 6.4 mM $CuSO_4$, 6.2 mM Na_2MoO_4, and 174 mM ethylene diamine tetraacetic acid (EDTA).

Plasmid construction

The primers used in this study are shown in Additional file 1: Table S1. The *lcc9* expression cassette (P_{gpdA}-SP_{GlaA}-*lcc9*-T_{trpC}) was synthesized by Sangon Biotech (Shanghai) Co., Ltd, and delivered as recombinant vector pUC57-*lcc9*. Among them, the *lcc9* was

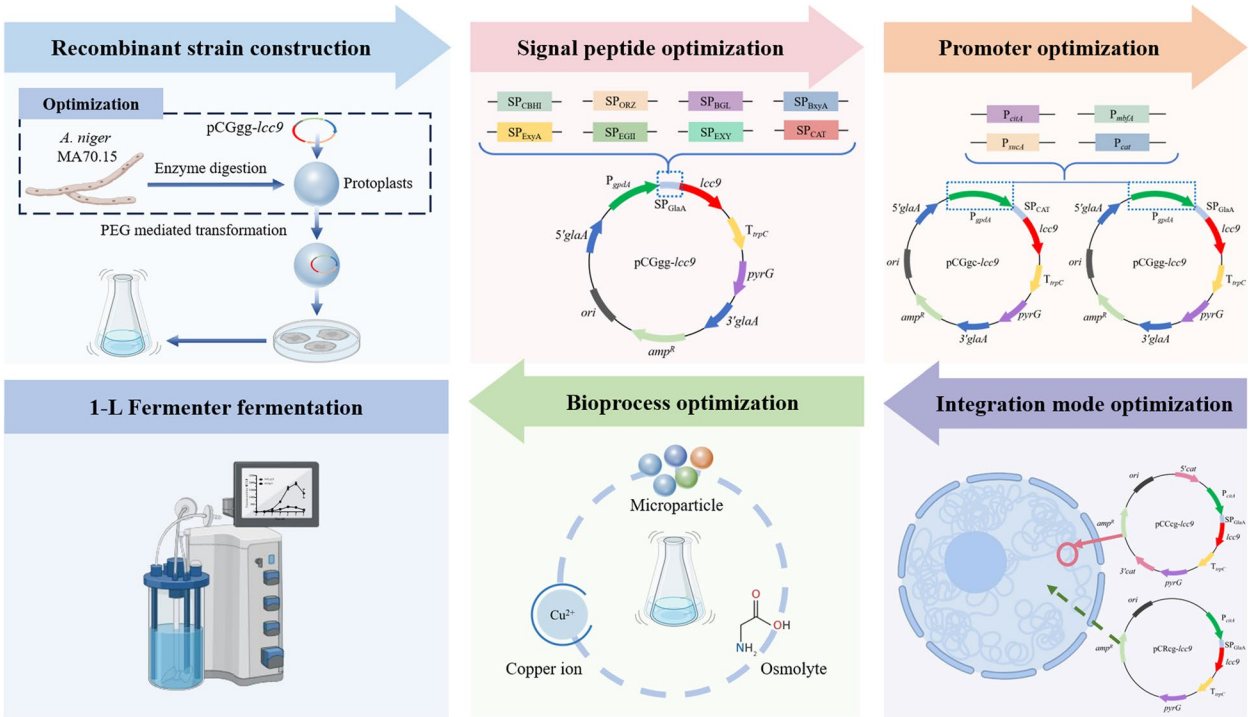

Fig. 1 Schematic diagram of the expression strategy used to enhance Lcc9 production

Table 1 Strains and plasmids used in this study

Strains or plasmids	Descriptions	References
Strains		
E. coli JM109	Clone strain	Takara
A. niger MA70.15	Δ*kusA*, Δ*pyrG*, clone strain	Our laboratory
AnGggL	*A.niger* MA70.15/pCGgg-*lcc9*, P_{gpdA}, SP_{GlaA}	This study
AnGgeL	*A.niger* MA70.15/pCGge-*lcc9*, P_{gpdA}, SP_{CBHI}	This study
AnGgoL	*A.niger* MA70.15/pCGgo-*lcc9*, P_{gpdA}, SP_{ORZ}	This study
AnGguL	*A.niger* MA70.15/pCGgu-*lcc9*, P_{gpdA}, SP_{BGL}	This study
AnGgxL	*A.niger* MA70.15/pCGgx-*lcc9*, P_{gpdA}, SP_{BxyA}	This study
AnGgnL	*A.niger* MA70.15/pCGgn-*lcc9*, P_{gpdA}, SP_{ExyA}	This study
AnGgdL	*A.niger* MA70.15/pCGgd-*lcc9*, P_{gpdA}, SP_{EGII}	This study
AnGgyL	*A.niger* MA70.15/pCGgy-*lcc9*, P_{gpdA}, SP_{EXY}	This study
AnGgcL	*A.niger* MA70.15/pCGgc-*lcc9*, P_{gpdA}, SP_{CAT}	This study
AnGccL	*A.niger* MA70.15/pCGcc-*lcc9*, P_{citA}, SP_{CAT}	This study
AnGscL	*A.niger* MA70.15/pCGsc-*lcc9*, P_{sucA}, SP_{CAT}	This study
AnGmcL	*A.niger* MA70.15/pCGmc-*lcc9*, P_{mbfA}, SP_{CAT}	This study
AnGacL	*A.niger* MA70.15/pCGac-*lcc9*, P_{cat}, SP_{CAT}	This study
AnGcgL	*A.niger* MA70.15/pCGcg-*lcc9*, P_{citA}, SP_{GlaA}	This study
AnGsgL	*A.niger* MA70.15/pCGsg-*lcc9*, P_{sucA}, SP_{GlaA}	This study
AnGmgL	*A.niger* MA70.15/pCGmg-*lcc9*, P_{mbfA}, SP_{GlaA}	This study
AnGagL	*A.niger* MA70.15/pCGag-*lcc9*, P_{cat}, SP_{GlaA}	This study
AnCcgL	*A.niger* MA70.15/pCCcg-*lcc9*, P_{citA}, SP_{GlaA}	This study
AnRcgL1	*A.niger* MA70.15/pCRcg-*lcc9*, P_{citA}, SP_{GlaA}	This study
Plasmids		
pC3	Recombinant expression vector backbone, *pyrG*	Our laboratory
pUC57-*lcc9*	amp^R (*E. coli*), *lcc9*	Sangon Biotech
pUC57-SP_{CBHI}	amp^R (*E. coli*), SP_{CBHI}	Our laboratory
pUC57-SP_{ORZ}	amp^R (*E. coli*), SP_{ORZ}	Our laboratory
pUC57-SP_{BxyA}	amp^R (*E. coli*), SP_{BxyA}	Our laboratory
pUC57-SP_{BGL}	amp^R (*E. coli*), SP_{BGL}	Our laboratory
pUC57-SP_{ExyA}	amp^R (*E. coli*), SP_{ExyA}	Our laboratory
pUC57-SP_{EGII}	amp^R (*E. coli*), SP_{EGII}	Our laboratory
pUC57-SP_{EXY}	amp^R (*E. coli*), SP_{EXY}	Our laboratory
pUC57-SP_{CAT}	amp^R (*E. coli*), SP_{CAT}	Our laboratory
pCGgg-*lcc9*	pC3 derivative, pC3-5′*glaA*-P_{gpdA}-SP_{GlaA}-*lcc9*-T_{trpC}-*pyrG*-3′*glaA*	This study
pCGge-*lcc9*	pC3 derivative, pC3-5′*glaA*-P_{gpdA}-SP_{CBHI}-*lcc9*-T_{trpC}-*pyrG*-3′*glaA*	This study
pCGgo-*lcc9*	pC3 derivative, pC3-5′*glaA*-P_{gpdA}-SP_{ORZ}-*lcc9*-T_{trpC}-*pyrG*-3′*glaA*	This study
pCGgu-*lcc9*	pC3 derivative, pC3-5′*glaA*-P_{gpdA}-SP_{BGL}-*lcc9*-T_{trpC}-*pyrG*-3′*glaA*	This study
pCGgx-*lcc9*	pC3 derivative, pC3-5′*glaA*-P_{gpdA}-SP_{BxyA}-*lcc9*-T_{trpC}-*pyrG*-3′*glaA*	This study
pCGgn-*lcc9*	pC3 derivative, pC3-5′*glaA*-P_{gpdA}-SP_{ExyA}-*lcc9*-T_{trpC}-*pyrG*-3′*glaA*	This study
pCGgd-*lcc9*	pC3 derivative, pC3-5′*glaA*-P_{gpdA}-SP_{EGII}-*lcc9*-T_{trpC}-*pyrG*-3′*glaA*	This study
pCGgy-*lcc9*	pC3 derivative, pC3-5′*glaA*-P_{gpdA}-SP_{EXY}-*lcc9*-T_{trpC}-*pyrG*-3′*glaA*	This study
pCGgc-*lcc9*	pC3 derivative, pC3-5′*glaA*-P_{gpdA}-SP_{CAT}-*lcc9*-T_{trpC}-*pyrG*-3′*glaA*	This study
pCGcc-*lcc9*	pC3 derivative, pC3-5′*glaA*-P_{citA}-SP_{CAT}-*lcc9*-T_{trpC}-*pyrG*-3′*glaA*	This study
pCGsc-*lcc9*	pC3 derivative, pC3-5′*glaA*-P_{sucA}-SP_{CAT}-*lcc9*-T_{trpC}-*pyrG*-3′*glaA*	This study
pCGmc-*lcc9*	pC3 derivative, pC3-5′*glaA*-P_{mbfA}-SP_{CAT}-*lcc9*-T_{trpC}-*pyrG*-3′*glaA*	This study
pCGac-*lcc9*	pC3 derivative, pC3-5′*glaA*-P_{cat}-SP_{CAT}-*lcc9*-T_{trpC}-*pyrG*-3′*glaA*	This study
pCGcg-*lcc9*	pC3 derivative, pC3-5′*glaA*-P_{citA}-SP_{GlaA}-*lcc9*-T_{trpC}-*pyrG*-3′*glaA*	This study
pCGsg-*lcc9*	pC3 derivative, pC3-5′*glaA*-P_{sucA}-SP_{GlaA}-*lcc9*-T_{trpC}-*pyrG*-3′*glaA*	This study
pCGmg-*lcc9*	pC3 derivative, pC3-5′*glaA*-P_{mbfA}-SP_{GlaA}-*lcc9*-T_{trpC}-*pyrG*-3′*glaA*	This study

Table 1 (continued)

Strains or plasmids	Descriptions	References
pCGag-*lcc9*	pC3 derivative, pC3-5′*glaA*-P_{cat}-SP_{GlaA}-*lcc9*-T_{trpC}-*pyrG*-3′*glaA*	This study
pCCcg-*lcc9*	pC3 derivative, pC3-5′*cat*-P_{citA}-SP_{GlaA}-*lcc9*-T_{trpC}-*pyrG*-3′*cat*	This study
pCRcg-*lcc9*	pC3 derivative, pC3-P_{citA}-SP_{GlaA}-*lcc9*-T_{trpC}-*pyrG*	This study

derived from *C. cinerea* okayama7#130 (Genome accession number: GCA_000182895.1) and optimized according to *A. niger* codon usage preferences. The SP_{GlaA} was derived from *A. niger* MA70.15 glucoamylase. The promoter P_{gpdA} and terminator T_{trpC} are derived from *A. nidulans*.

The P_{gpdA}-SP_{GlaA}-*lcc9*-T_{trpC} fragment was obtained from pUC57-*lcc9* using primers P_{gpdA}-F/T_{trpC}-R. The *pyrG* was obtained from pC3 using primers *pyrG*-F/*pyrG*-R. The *glaA* homology arms 5′*glaA* and 3′*glaA* fragments were obtained from the *A. niger* MA70.15 mycelium using primers 5′*glaA*-F/5′*glaA*-R and 3′*glaA*-F/3′*glaA*-R, respectively. Then, the 5′*glaA*-P_{gpdA}-SP_{GlaA}-*lcc9*-T_{trpC}-*pyrG*-3′*glaA* fragment was constructed by overlap PCR. The pC3 fragment (the backbone of pCGgg-*lcc9*) was obtained from pC3 using primers pC3-F/pC3-R. The plasmid pCGgg-*lcc9* was created by linking the 5′*glaA*-P_{gpdA}-SP_{GlaA}-*lcc9*-T_{trpC}-*pyrG*-3′*glaA* fragment with the pC3 fragment using the One Step Cloning Kit (Vazyme, Nanjing, China).

The pCGg-*lcc9* fragment (the backbone of pCGge-*lcc9*) was obtained from plasmid pCGgg-*lcc9* using primers pCGgg-*lcc9*-F/pCGgg-*lcc9*-R. The SP_{CBHI}, SP_{ORZ}, SP_{BxyA}, SP_{BGL}, SP_{ExyA}, SP_{EGII}, SP_{EXY}, and SP_{CAT} were obtained from pUC57-SP_{CBHI}, pUC57-SP_{ORZ}, pUC57-SP_{BxyA}, pUC57-SP_{BGL}, pUC57-SP_{ExyA}, pUC57-SP_{EGII}, pUC57-SP_{EXY}, and pUC57-SP_{CAT} using primers SP-F1/SP-R1, SP-F2/SP-R2, SP-F3/SP-R3, SP-F4/SP-R4, SP-F5/SP-R5, SP-F6/SP-R6, SP-F7/SP-R7, and SP-F8/SP-R8, respectively. The plasmids pCGge-*lcc9*, pCGgo-*lcc9*, pCGgu-*lcc9*, pCGgx-*lcc9*, pCGgn-*lcc9*, pCGgd-*lcc9*, pCGgy-*lcc9*, and pCGgc-*lcc9* were obtained by linking the SP_{CBHI}, SP_{ORZ}, SP_{BxyA}, SP_{BGL}, SP_{ExyA}, SP_{EGII}, SP_{EXY}, and SP_{CAT} with the pCGg-*lcc9* fragment using the One Step Cloning Kit, respectively.

The pCGc-*lcc9* fragment (the backbone of pCGcc-*lcc9*) was obtained from plasmid pCGgc-*lcc9* using primers Vector-F1/Vector-R1. The P_{citA}, P_{sucA}, P_{mbfA}, and P_{cat} fragments were obtained from the *A. niger* MA70.15 genome using primers Pro-F1/Pro-R1, Pro-F2/Pro-R2, Pro-F3/Pro-R3 and Pro-F4/Pro-R4, respectively. The plasmids pCGcc-*lcc9*, pCGsc-*lcc9*, pCGmc-*lcc9*, and pCGac-*lcc9* were obtained by linking the pCGc-*lcc9* fragment with the P_{citA}, P_{sucA}, P_{mbfA}, and P_{cat} fragments, respectively, using the One Step Cloning Kit.

The pCGg-*lcc9* fragment (the backbone of pCGcg-*lcc9*) was obtained from plasmid pCGgg-*lcc9* using primers Vector-F2/Vector-R2. The P_{citA}, P_{sucA}, P_{mbfA}, and P_{cat} fragments were obtained from the *A. niger* MA70.15 genome using primers Pro-F5/Pro-R5, Pro-F6/Pro-R6, Pro-F7/Pro-R7 and Pro-F8/Pro-R8, respectively. The vectors pCGcg-*lcc9*, pCGsg-*lcc9*, pCGmg-*lcc9*, and pCGag-*lcc9* were obtained by linking the P_{citA}, P_{sucA}, P_{mbfA}, and P_{cat} with the pCGc-*lcc9* fragment using the One Step Cloning Kit, respectively.

The homology arms 5′*cat* and 3′*cat* fragments were obtained from the *A. niger* MA70.15 mycelium using primers 5′*cat*-F/5′*cat*-R and 3′*cat*-F/3′*cat*-R, respectively. The P_{citA}-SP_{GlaA}-*lcc9*-T_{trpC}-*pyrG* fragment was obtained from the pCGcg-*lcc9* using primers loci-F1/loci-R1. Then, the 5′*cat*-P_{citA}-SP_{GlaA}-*lcc9*-T_{trpC}-*pyrG*-3′*cat* fragment was constructed by overlap PCR. The pCCcg-*lcc9* fragment (the backbone of pCCcg-*lcc9*) was obtained from plasmid pCGcg-*lcc9* using primers loci-F2/loci-R2. The plasmid pCCcg-*lcc9* was created by linking the 5′*cat*-P_{citA}-SP_{GlaA}-*lcc9*-T_{trpC}-*pyrG*-3′*cat* fragment with the pCCcg-*lcc9* fragment using the One Step Cloning Kit.

The pCRcg-*lcc9* fragment (the backbone of pCRcg-*lcc9*) was obtained from plasmid pCGcg-*lcc9* using primers loci-F4/loci-R4. The P_{citA}-SP_{GlaA}-*lcc9*-T_{trpC}-*pyrG* fragment was obtained from the pCGcg-*lcc9* using primers loci-F3/loci-R3. The plasmid pCRcg-*lcc9* was created by linking the P_{citA}-SP_{GlaA}-*lcc9*-T_{trpC}-*pyrG* fragment with the pCRcg-*lcc9* fragment using the One Step Cloning Kit.

Construction and validation of *A. niger* transformants

The *A. niger* MA70.15 was cultivated on a PDA plate at 28 ℃ for 5 d, after which four fungal plugs of *A. niger* with a diameter of 5 mm were added to YPD medium and incubated at 30 ℃, 200 rpm for 48 h. When culturing the Δ*pyrG* strain, 10 mM uracil must be added to the medium. Subsequently, fresh mycelium was harvested through suction filtration and subjected to a 3 h digestion process with an enzyme cocktail (2% cellulase + 1% snailase) in a water bath shaker at 30 ℃, 100 rpm for 3 h to obtain fresh protoplasts for transformation. In the protoplast preparation optimization process, the cellulase, lyticase, and lysozyme used were purchased from Acmec Biochemical Technology (Shanghai) Co., Ltd., and

the snailase used was purchased from Sangon Biotech (Shanghai) Co., Ltd.

The plasmid (4–10 μg) was added to 200 μL of protoplasts obtained from *A. niger*. Subsequently, 50 μL PEG solution (60% PEG, 50 mM $CaCl_2$, and 10 mM Tris HCl, pH 7.5) was added, and the mixture was incubated on ice for 30 min. After that, the mixture was further incubated in a PEG solution at room temperature for another 25 min. Finally, the transformants were cultured in a high osmolarity CD agar medium at 28 ℃ for protoplast regeneration.

Transformants were selected for uracil prototrophy by growth on a selective solid minimal medium (without uracil) and the *lcc9* expression cassette was verified to be integrated into the transformant genome by diagnostic PCR using primers F1/R1. As the host strain *A. niger* MA70.15 is *kusA*-deficient, the transformed plasmid will achieve targeted integration into the genome through the homologous arm. To verify that the target fragment was successfully integrated into the *glaA* locus and that the transformants were homokaryotic, primers F2/R2 were designed using upstream sequences of the *glaA* locus and intra-*glaA* integration deletion sequences as templates, respectively. The schematic of the above verification process is shown in Fig. 2A. A similar principle applies to the validation of positive transformants with integrated expression at the *cat* locus. Among them, primers F3/R3 were designed using upstream sequences of the *cat* locus and intra-*cat* integration deletion sequences as templates, respectively.

To obtain genome sequence information of *A. niger*, mycelium was collected after culturing in shake flasks for 5 d and then sent to Shanghai OE Biotech Co., Ltd. for whole genome denovo sequencing.

Bioprocess optimization

Microparticle type and concentration optimization

The microparticles ($CaCO_3$, $MgSiO_3$, and Al_2O_3) were separately suspended in 50 mM sodium acetate buffer (pH 6.5) and autoclaved at 121 ℃ for 20 min.

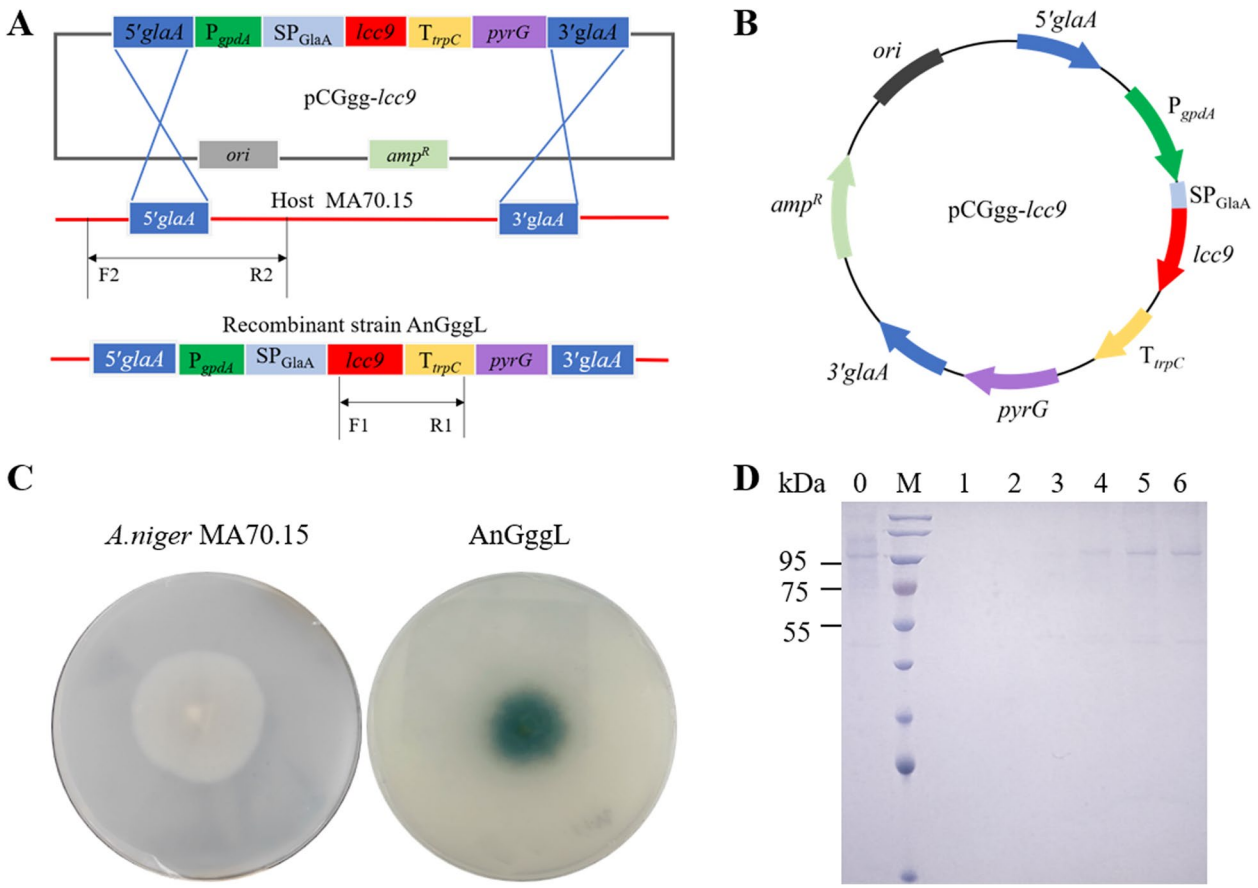

Fig. 2 Recombinant extracellular production of *lcc9* in *A. niger*. **A** Genomic loci-specific integration diagram of *lcc9* expression cassette. **B** Schematic structure of the plasmid pCGgg-*lcc9*. **C** *A.niger* MA70.15 and AnGggL laccase activity detection based on plates containing ABTS. **D** SDS-PAGE analysis of *A.niger* MA70.15 and AnGggL fermentation supernatant. M: protein molecular weight marker; Lane 0: fermentation supernatant samples from MA70.15 shake flasks cultured for 6 d; Lanes 1–6: fermentation supernatant samples from AnGggL shake flasks cultured for 1–6 d, respectively

The microparticles were then added to the fermentation medium at a concentration of 0.5% (w/v). Different additive concentrations of 0.5%, 1%, and 2% were then selected to investigate the effect of microparticle concentration on laccase activity.

Osmolyte type and concentration optimization

Glycine, proline, and trimethylamine oxide (TMAO) were added to the fermentation medium at a concentration of 0.2 M, respectively. To further investigate the effect of osmolyte concentration on laccase activity, different addition concentrations were selected. The glycine was added at concentrations of 0.05, 0.1, 0.2, 0.3, and 0.4 M, respectively; and the proline was added at concentrations of 0.1, 0.2, 0.3, 0.4, and 0.5 M, respectively.

Cu^{2+} concentration optimization

Cu^{2+} was added to the fermentation medium at concentrations of 0.1, 0.5, 1, 2, 3, and 4 mM, respectively. Note that the trace element added to the fermentation medium contains Cu^{2+} and the Cu^{2+} are added here in addition.

Shake flask and 1-L fermenter cultivation

The spore solution stored in the -80 ℃ refrigerator was inoculated onto PDA plates for activation, after which they were again transferred to PDA plates for conidia production at 28 ℃ for 5 d. The spore suspension was obtained by washing the PDA plate with a solution containing 0.9% NaCl and 0.05% Tween 80. The above spore suspension was then transferred to a 500-mL triangular flask containing 100 mL fermentation medium according to an inoculum volume of 1×10^5 spores/mL, and cultured at 30 ℃ and 200 rpm.

Referring to spore suspension preparation and inoculum volume in shake flask fermentation, the obtained spore suspension was transferred to a 1-L fermenter (Baoxing Bio-Engineering, Biotech-JS/JSA-1L) containing 1 L fermentation medium and incubated at 30 ℃, pH 5.5, 200 rpm with an airflow rate of 50 L/h. The airflow rate was maintained at 20 L/h from the 2nd day after inoculation. During the above fermentation process, samples were taken every 24 h and centrifuged at 12,000 × *g* for 10 min at 4 ℃ to obtain culture supernatants for subsequent laccase expression assays.

Mycelial morphology observation

To investigate the effect of growth environment optimization on mycelial morphology, individual mycelial pellets or clusters were selected from the fermentation system after shaking flask incubation, blotted dry with filter paper, and observed microscopically at 10x magnification.

Laccase activity determination and protein gel electrophoresis analysis

Laccase activity was determined according to the method reported by Kai Pan et al. [22]. Briefly, 17 μL of fermentation supernatant was mixed with 33 μL of ABTS (15 mM) and 950 μL of sodium tartrate buffer (pH 4.0, 100 mM). The mixture was reacted in a 30 ℃ water bath for 3 min and then cooled in ice water. Its absorbance value was measured at 420 nm. One activity unit (U) was defined as the amount of laccase required for oxidizing 1 μM of ABTS per minute. The formula for laccase activity calculation is $OD_{420} \times$ dilution factor $\times 555.56$ (U/L).

SDS-PAGE and native-PAGE of laccase were performed according to the method reported by Juanjuan Liu et al. [24] and Ganfei Xu et al. [25], respectively. The sample volume for both SDS-PAGE and native-PAGE analysis was 15 μL. After electrophoresis, the denatured gel was stained with Coomassie Brilliant Blue R-250, and the active gel was immersed in 100 mM citrate phosphate buffer containing 15 mM ABTS, then incubated at 30 ℃ until a green band appeared. The original images corresponding to all the native-PAGE in this study are shown in Additional file 2.

For peptide fingerprinting detection of the protein band, the target strip in the SDS-PAGE was cut and sent to Sangon Biotech (Shanghai) Co., Ltd. under low-temperature preservation for experiments and data analysis.

Quantitative reverse transcription-PCR (qRT-PCR) analysis

A. niger mycelia were harvested by centrifugation of fermentation broth samples at 12,000 × *g* for 10 min at 4 ℃. Then their total RNA and corresponding cDNA were obtained using RNAiso-Plus extraction reagent (TaKaRa, Dalian, China) and Evo M-MLV RT kit (AG, Hunan, China), respectively. The obtained cDNA was used as a template for qRT-PCR, and the transcription level of *lcc9* was determined with the *β-actin* as the reference gene. Primers used for qRT-PCR amplification of the *lcc9* and *β-actin* are shown in Additional file 1: Table S1. qRT-PCR was performed based on the Light-Cycler 96 Real-Time PCR system (Roche, Basel, Switzerland) using the SYBR Green Premix Pro Taq HS qPCR Kit (AG, Hunan, China). qRT-PCR protocols were set following the instructions from the Premix *Pro Taq* HS qPCR Kit (AG, Hunan, China) manufacturer. The data were analyzed using $2^{-\Delta\Delta CT}$ methodology [26].

Statistical analysis

All data were obtained through three independent experiments and presented as the averages ± standard deviation. The SAS statistical software (version 8.1, SAS Institute Inc., Cary, NC, USA) was used to perform

statistical analysis. Data were statistically analyzed using Student's *t*-test and $p < 0.05$ was considered a statistically significant difference.

Results and discussion

Recombinant extracellular production of Lcc9 in *A. niger*

The vector pCGgg-*lcc9* (Fig. 2B) containing *lcc9* was transformed into *A. niger* MA70.15 to obtain the recombinant strain AnGggL. The naming convention for AnGggL is as follows: the first two letters represent *A. niger*, the third letter indicates the integration region *glaA* locus, the fourth letter represents the promoter P_{gpdA}, the fifth letter indicates the signal peptide SP_{GlaA} and the last letter represents laccase *lcc9*. When cultured on CD plates containing ABTS, The AnGggL can form a green halo (Fig. 2C). However, no laccase activity was detected in the fermentation supernatant of AnGggL after shake flask cultivation, and no Lcc9 (~59 kDa) protein bands were observed in the SDS-PAGE (Fig. 2D) and native-PAGE (data not shown) results of the corresponding samples. The above results indicate that although AnGggL can achieve recombinant extracellular production of Lcc9, the production level is low.

In previous studies, recombinant expression of laccase SlLac2 and PsLac2 derived from *Stemphylium lucomagnoense* and *Pestalotiopsis* sp. in *A. niger* resulted in extracellular laccase activities of 85.9 and 15.12 nkat/mL, with approximately 5154 and 907 U/L, respectively [10, 27]. Differences between the results of this study and those of the above studies may be due to variations in factors such as gene expression cassettes, integration locus, and culture conditions of the recombinant strains.

In addition, it is noted that a protein band near 95 kDa appeared in the SDS-PAGE results of *A. niger* MA70.15 and AnGggL extracellular supernatants (Fig. 2D). The protein was identified by peptide fingerprinting as catalase (Additional file 1: Fig. S1). Previous studies have shown that promoters and signal peptides commonly used in the *Brevibacillus brevis* expression system are derived from expression regulatory elements corresponding to its high extracellular abundance protein HWP [28]. Moreover, integrating the *lacA* expression cassette into the gene locus encoding the extracellular high abundance protein CBHI in the *Trichoderma reesei* genome enables efficient extracellular expression of laccase LacA [29]. These results suggest that expression regulatory elements and genomic loci of genes encoding extracellular high abundance proteins in the chassis host genome can be used for efficient extracellular expression of recombinant proteins. Inspired by this, subsequent studies will investigate whether the signal peptide and promoter based on the identified catalase gene as well as its genomic locus can increase the recombinant extracellular production level of Lcc9 in *A. niger*.

Another problem we noticed in this part of the project is the low transformation efficiency of *A. niger* MA70.15 (5 transformants/μg DNA). Therefore, to facilitate the implementation of subsequent expression strategies, we will first establish an efficient genetic transformation system for *A. niger* MA70.15.

A. niger protoplast preparation optimization

Quantity and quality of protoplast preparation are important factors affecting the efficiency of *A. niger* transformation using the PMT method [4]. Therefore, to improve the genetic transformation efficiency of *A. niger* MA70.15, we optimized the protoplast preparation conditions, including cell wall digestion enzyme mixture, incubation time, incubation temperature, and mycelium age.

The composition of the cell wall digestion enzyme solution can directly affect the effectiveness of mycelial cell wall cleavage and is a key factor in obtaining high yields of protoplasts [30]. Here, four types of cell wall digestion enzymes, including cellulase, snailase, lyticase, and lysozyme, were used individually or in combination to prepare protoplasts. As shown in Fig. 3A, *A. niger* mycelium treated with an enzyme solution containing 2% cellulase, 1% snailase, 1% lyticase, and 0.5% lysozyme produced the highest number of protoplasts with a density of 9.9×10^5 protoplasts/mL, whereas no protoplasts were produced with 2% cellulase alone. *A. niger* cell wall polysaccharides are complex structures composed of chitin, cellulose, and dextran [31], which may be an important reason why a single cellulase could not be used to obtain protoplasts in this study. Similarly, it has been previously reported that only a very limited amount of protoplasts could be obtained from *A. niger* ATCC 20611 mycelium despite using varying concentrations of individual digestion enzymes [6].

Selecting an appropriate incubation time is also necessary to obtain a sufficient number of high-quality protoplasts, as too short or too long incubation of the mycelium with the enzymatic solution will result in incomplete protoplast release or degradation of early protoplasts. The mycelium was incubated with the optimal cell wall enzymatic solution (2% cellulase, 1% snailase, 1% lyticase, and 0.5% lysozyme) for 3.5 h. Samples were taken every half hour to determine the number of prepared protoplasts. The results showed that it reached a maximum value of 1×10^6 protoplasts/mL after incubation for 3 h, which is 9-fold higher than that at 1.5 h (Fig. 3B).

In addition, the incubation temperature affects the protoplast release efficiency by influencing the digestion

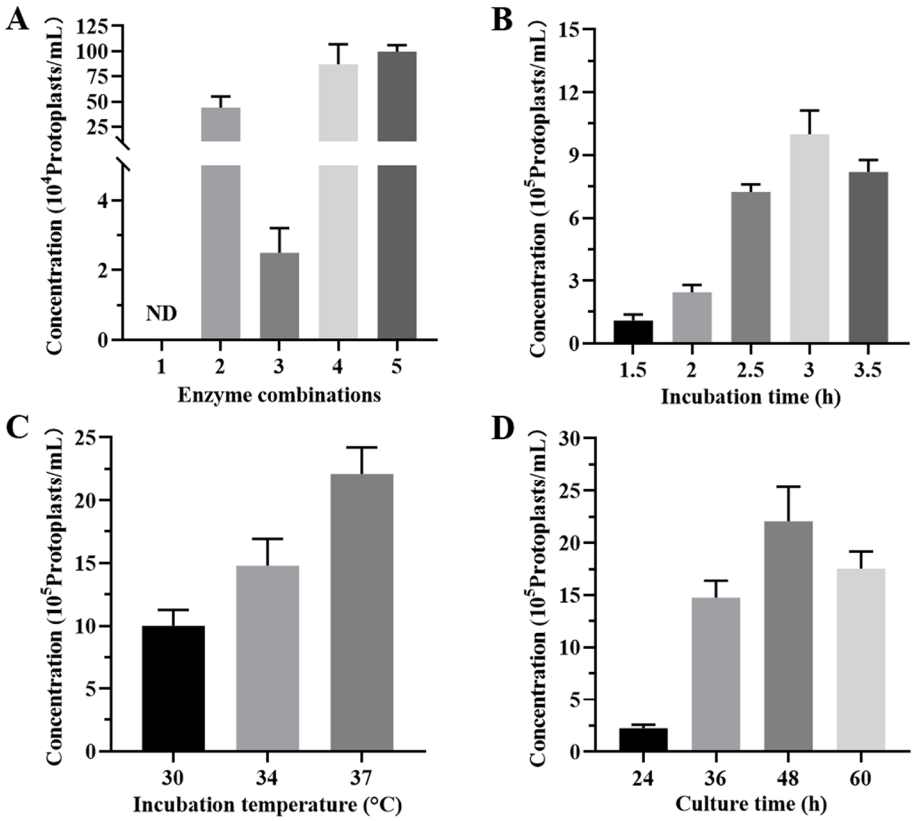

Fig. 3 *A.niger* MA70.15 protoplast preparation system optimization. **A** Protoplast production with different enzymatic combinations. 1: 2% cellulase; 2: 2% cellulase + 1% snailase; 3: 2% cellulase + 1% lyticase; 4: 2% cellulase + 1% snailase + 1% lyticase; 5: 2% cellulase + 1% snailase + 1% lyticase + 0.5% lysozyme. **B** Protoplast production with different incubation times. **C** Protoplast production with different incubation temperatures. **D** Protoplast production with different mycelial ages. Error bars represent the standard deviation

enzyme activity. Therefore, we set three incubation temperatures (30, 34, and 37 ℃) to explore the optimal incubation temperature based on the optimal incubation time and lytic enzyme combination. As shown in Fig. 3C, the number of protoplasts could be increased 2.2-fold to 2.2×10^6 protoplasts/mL when the incubation temperature was 37 ℃.

Mycelium age is also an important factor in protoplast preparation because the size and solid density of mycelium pellets formed vary at different incubation times, which indirectly affects enzymatic digestion [4]. Mycelia cultured for 24, 36, 48, and 60 h were selected for protoplast preparation, respectively. It was found that as the mycelium age increased, the number of protoplasts obtained first increased and then decreased, reaching a maximum at 48 h (Fig. 3D).

To summarize, the optimal conditions for producing *A. niger* MA70.15 protoplasts in this study were as follows: mycelia were cultured for 48 h and then incubated for 3 h at 37 ℃ in an enzyme solution containing 2% cellulase, 1% snailase, 1% lyticase, and 0.5% lysozyme. The final yield of protoplasts obtained was 2.2×10^6 protoplasts/mL. Based on the protoplasts prepared under the above conditions, the plasmid pCGgg-*lcc9* transformation efficiency obtained was 19 transformants per μg DNA, which is 3.8-fold higher than that before optimization. Liu et al. obtained *A. niger* N1 and O1 transformation efficiencies of 28 and 39 transformants per 10 μg DNA, respectively, by optimizing protoplast preparation conditions [5]. Since transformation efficiency also depends on factors such as osmotic stabilizer and PEG solution, as well as the strain used in the transformation system, it is reasonable to assume that the discrepancy between the results of the present study and those of Liu et al. could be due to differences in overall operating procedure and preparation system.

Effect of signal peptide element on Lcc9 production

Signal peptides are N-terminal specific sequences of intracellular protein precursors that play an important role in translation initiation and extracellular secretion of target proteins [32]. To enhance extracellular Lcc9 expression, we selected seven signal peptides (SP_{CBHI}, SP_{ORZ}, SP_{BxyA}, SP_{BGL}, SP_{ExyA}, $SP_{EGII,}$ and SP_{EXY}) that can

mediate target proteins to achieve efficient expression in *A. niger*, based on a literature review [9, 33, 34]. In addition, we investigated the effect of the signal peptide of the extracellular high abundance protein catalase (SP_{CAT}) from *A. niger* MA70.15 on Lcc9 expression. Sequence information for the above signal peptides is provided in Additional file 1: Table S2.

To exclude the influence of protoplast preparation method on the recombinant extracellular expression of Lcc9, we reconstructed the recombinant strain based on the optimal protoplast preparation system and plasmid pCGgg-*lcc9* at this experimental stage. It was found that the protoplast optimization process did not affect the recombinant extracellular expression of Lcc9 in *A. niger* MA70.15 (data not shown). After incubation on plates containing ABTS, it was observed that all *A. niger* recombinant strains mediated by the above eight signal peptides could produce a green halo, with the SP_{CAT}-mediated AnGgcL (containing P_{gpdA}-SP_{CAT}) requiring the shortest time, only 2–3 d, while the other strains required 8–10 d (Additional file 1: Fig. S2). After 5 d of shake flask cultivation, the extracellular laccase activity of AnGgcL reached 10 U/L, and the corresponding fermentation supernatant sample showed a clear green band in the native-PAGE (Additional file 1: Fig. S3A). On the contrary, the corresponding fermentation supernatant sample from *A. niger* MA70.15, which served as a negative control, showed no obvious green bands in Native-PAGE (Additional file 1: Fig. S3B). These results indicate that the SP_{CAT} identified in this study is the optimal signal peptide to mediate the recombinant extracellular expression of Lcc9 in *A. niger* MA70.15. To our knowledge, this is the first report of the SP_{CAT} application in *A. niger* expression system.

SP_{GlaA}, one of the signal peptides widely used in the *A. niger* expression system [35], mediates the extracellular SlLac2 activity in *A. niger* up to 85.9 nkat/mL (~ 5154 U/L) after 9 d of shake flask cultivation [10]. However, no laccase activity was detected in the shake flask fermentation supernatant of AnGggL (containing P_{gpdA}-SP_{GlaA}) mediated by SP_{GlaA} in this study (data not shown). This may be due to variations in laccase sequences, promoters, and chassis hosts used in different studies.

Effect of promoter element on Lcc9 production

Promoters are important expression regulatory elements that control transcription initiation and intensity of target genes [36]. Based on AnGgcL (containing P_{gpdA}-SP_{CAT}), we investigated the effects of three promoters with high transcriptional activity in the *A. niger* expression system, namely P_{citA} [37], P_{sucA} [12], and P_{mbfA} [11], as well as the catalase gene promoter (P_{cat}), on the recombinant expression of Lcc9. The sequence information of the above promoters is shown in Additional file 1: Table S3. Given the relatively wide application of SP_{GlaA} in the *A. niger* expression system [9], we also performed corresponding promoter optimization studies based on AnGggL (containing P_{gpdA}-SP_{GlaA}). Eight recombinant expression strains of *lcc9* mediated by different promoters and signal peptides were finally obtained, namely AnGccL (containing P_{citA}-SP_{CAT}), AnGscL (containing P_{sucA} -SP_{CAT}), AnGmcL (containing P_{mbfA} -SP_{CAT}), AnGacL (containing P_{cat}-SP_{CAT}), AnGcgL (containing P_{citA}-SP_{GlaA}), AnGsgL (containing P_{sucA}-SP_{GlaA}), AnGmgL (containing P_{mbfA}-SP_{GlaA}) and AnGagL (containing P_{cat}-SP_{GlaA}) (Table 1).

All of the above recombinant strains formed green halos after cultivation on plates containing ABTS, with AnGscL, AnGmcL, and AnGcgL taking only 2–3 d, while the other strains required 8–10 d (Additional file 1: Fig. S4). However, after shaking flask cultivation for 5 d, laccase activity was detected only in the fermentation supernatant of AnGcgL (containing P_{citA}-SP_{GlaA}), which was 20 U/L, while the other strains remained undetectable. Native-PAGE results displayed similar patterns to the enzyme activity (Fig. 4A). In addition, qRT-PCR analysis of the obtained recombinant strains showed that the *lcc9* were all successfully transcribed, with the highest transcription level in the AnGggL (containing P_{gpdA}-SP_{GlaA}) strain (Fig. 4B). This is similar to many previous reports in which the extracellular activity of target proteins did not match the intracellular transcript levels of their encoded genes [38]. This may be attributed to the fact that beyond the intracellular mRNA content, post-transcriptional translation and secretion efficiency also play an important role in the extracellular expression of target proteins.

A. niger is an important producer of citric acid in industry, and citrate synthase is active throughout its growth. It has been shown that the citrate synthase gene promoter P_{citA} can initiate efficient transcription of *mCherry-pyrG* at different developmental stages of *A. niger* [37]. Similarly, P_{citA}-mediated AnGcgL had the highest extracellular laccase activity in this study. Interestingly, despite using the same promoter P_{citA}, AnGccL (containing P_{citA}-SP_{CAT}) and AnGcgL (containing P_{citA}-SP_{GlaA}) exhibited different extracellular laccase activities, indicating that signal peptide and promoter compatibility may be necessary to achieve efficient extracellular expression of Lcc9. Optimizing promoter-signal peptide compatibility has also been shown in previous studies to be an effective strategy for increasing target protein expression levels. For example, the promoters P_{glaA}, P_{amyA}, and P_{ammA} were combined with the signal peptides SP_{GlaA}, SP_{AmyA}, and SP_{AmmA}, respectively, and it was found that the extracellular xylanase activity varied significantly with the combination. Among them, the xylanase activity mediated by

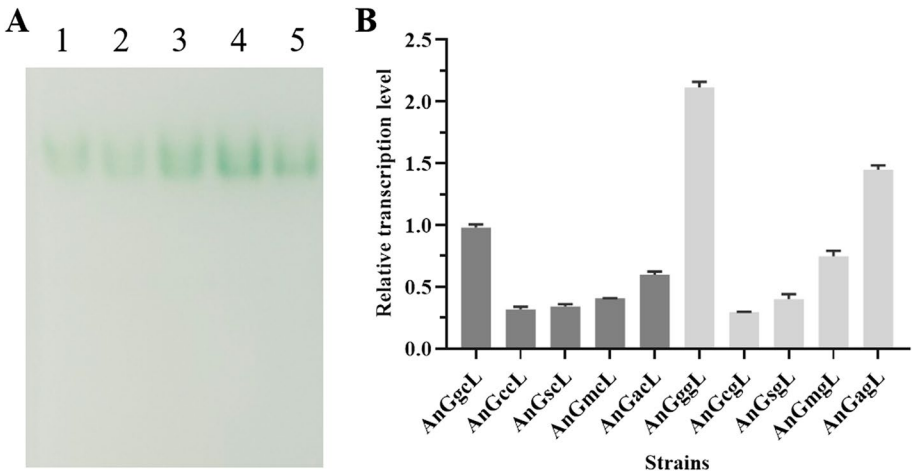

Fig. 4 Effect of promoter optimization on the extracellular Lcc9 production. **A** Native-PAGE analysis of AnGcgL fermentation supernatant. Lanes 1–5: supernatant samples of AnGcgL at 2, 3, 4, 5, and 6 d, respectively. **B** Relative transcription levels of *lcc9* in *A.niger* strains. Error bars represent the standard deviation

P_{glaA}-SP_{AmyA} was approximately 1.3-fold higher than that of P_{ammA}-SP_{AmyA} [39]. Since the AnGcgL containing the P_{citA}-SP_{GlaA} had the highest extracellular laccase activity, subsequent studies were based on it alone.

Effect of integration mode on Lcc9 production

It is well known that in genomic integration, the target gene expression cassette integration loci have an obvious "positional effect" on target protein expression [40]. Therefore, in addition to integrating the *lcc9* expression cassette into the *A. niger* MA70.15 genomic *glaA* locus, we also investigated the effect of the catalase gene *cat* locus on the extracellular Lcc9 expression and explored other potentially efficient genomic loci by random integration.

In this regard, the vector pCCcg-*lcc9* (Additional file 1: Fig. S5) was transformed into *A. niger* MA70.15 to obtain recombinant strain AnCcgL, which integrated the *lcc9* expression cassette into the *cat* locus. The vector pCRcg-*lcc9* (Additional file 1: Fig. S5) was transformed into *A. niger* MA70.15 to obtain recombinant strains AnRcgL, which was randomized to integrate the *lcc9* expression cassette (a total of 20 positive transformants were obtained). We added identical amounts of DNA during random and targeted integration, both at 8 μg. At the same time, all factors remained consistent except for differences in the expression plasmids used in terms of whether or not they contained integration loci homologous arm sequences. Among these recombinant strains obtained based on the random integration model, only AnRcgL1 could show a visible green halo on plates containing ABTS within 2–3 d, while the other strains required more than 8 d (Additional file 1: Fig. S6). The extracellular laccase activity of AnRcgL1 reached 86 U/L after shake flask fermentation, and its

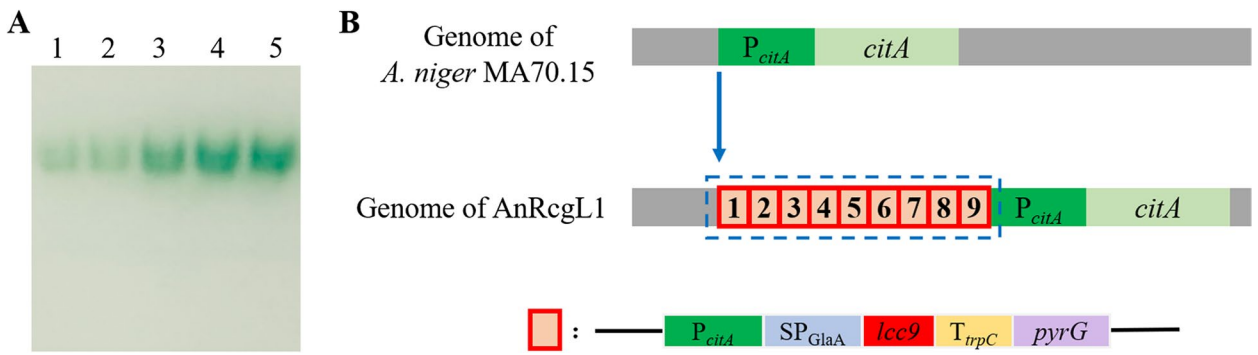

Fig. 5 AnRcgL1 production laccase activity assay and expression mechanism analysis. **A** Native-PAGE analysis of AnRcgL1 fermentation supernatant. Lanes 1–5: supernatant samples of AnRcgL1 at 2, 3, 4, 5, and 6 d, respectively. **B** Expression mechanism analysis of laccase production by AnRcgL1

fermentation supernatant samples showed significantly thickened protein bands in native-PAGE (Fig. 5A).

In previous studies to achieve efficient recombinant expression of target genes in *A. niger*, the corresponding gene expression cassettes were often integrated into a limited number of known high expression locus in the chassis host genome, such as glucoamylase, β-glucosidase, and α-amylase. However, due to the limited knowledge of current genomic information on *A. niger*, it is difficult to determine the potential of other gene loci in enhancing protein expression. Integrating target gene expression cassettes into the genome in a randomized integration mode is an effective solution to the above problems. For example, the marine-derived fungal laccase SlLac2 successfully achieved recombinant extracellular expression in *A. niger* by a randomized integration mode, and about 90% of the positive transformants exhibited laccase activity [10]. However, the specific information on the SlLac2 encoding gene integration locus was not further investigated.

In this study, integration of the *lcc9* expression cassette into the *cat* locus did not further increase the extracellular laccase activity compared to the *glaA* locus (Additional file 1: Fig. S6). This suggests that the *cat* locus is not suitable for efficient expression of the Lcc9. On the contrary, AnRcgL1 obtained by random integration had the highest extracellular laccase activity. To investigate the reasons for the increased extracellular laccase activity of AnRcgL1, whole genome sequencing was performed. The data showed that the *lcc9* expression cassette was integrated in nine consecutive copies into the promoter upstream region of the citrate synthase gene in the AnRcgL1 genome (Fig. 5B). This suggests that the combined effect of integration loci and copy number may be responsible for the increased extracellular laccase activity of AnRcgL1.

Effect of bioprocess on Lcc9 production

For filamentous fungi expression systems, mycelial morphology is also an important factor influencing

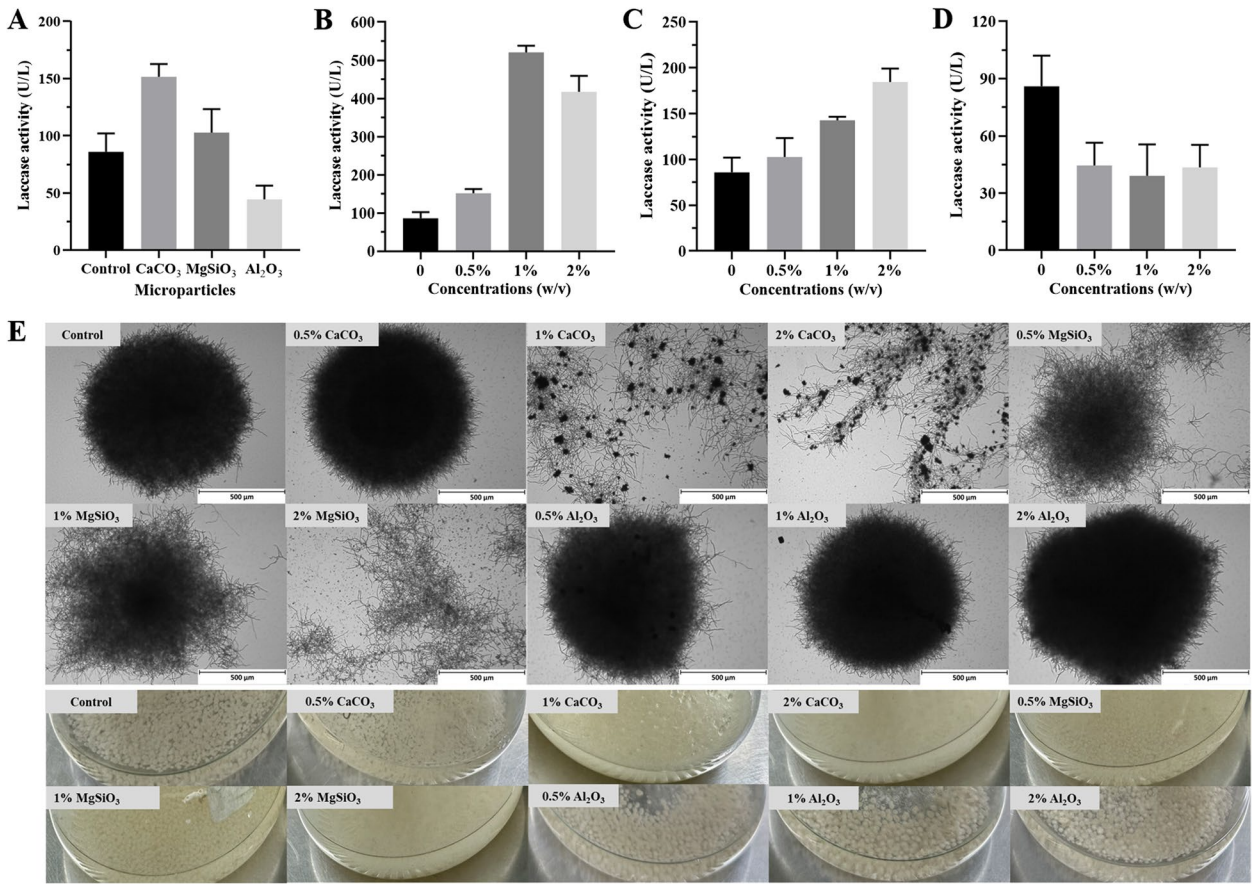

Fig. 6 Effect of microparticle optimization on the extracellular Lcc9 production. **A** Effect of different microparticle types. **B** Effect of varying the $CaCO_3$ concentration. **C** Effect of varying the $MgSiO_3$ concentration. **D** Effect of varying the Al_2O_3 concentration. **E** Effect of microparticles on *A. niger* mycelial morphology in shake flask fermentation. Error bars represent the standard deviation

recombinant protein expression levels. Filamentous fungi mycelial morphology can be regulated by genetic engineering modification and bioprocess optimization [4]. For example, microparticles in the fermentation medium are the key component affecting mycelial morphology [16]. In addition, osmolytes and metal ions in the fermentation medium can have an impact on target protein yields by directly or indirectly affecting their post-translational folding [19]. Therefore, based on the results of *lcc9* expression cassette optimization, we investigated the effects of microparticles, osmolytes, and Cu^{2+} in the culture medium on the extracellular laccase activity of AnRcgL1.

Effect of microparticle on Lcc9 production

In initial experiments, three types of microparticles ($CaCO_3$, $MgSiO_3$, and Al_2O_3) were added to the fermentation medium separately with a final concentration of 0.5% (w/v). As shown in Fig. 6A, the best microparticle source for Lcc9 production by AnRcgL1 was $CaCO_3$, followed by $MgSiO_3$, which increased extracellular laccase activity by 76% and 19%, respectively. However, adding Al_2O_3 reduced the extracellular laccase activity of AnRcgL1 by 48% (Fig. 6A).

Then, the effect of different microparticle addition concentrations (0.5%, 1%, and 2%) on extracellular laccase activity was investigated. Among them, AnRcgL1 extracellular laccase activity reached a maximum of 520.6 U/L at a $CaCO_3$ concentration of 1%, which was 6.05-fold higher than that without $CaCO_3$ (Fig. 6B). Although AnRcgL1 extracellular laccase activity shows a positive correlation with the $MgSiO_3$ concentration, the maximum selectable concentration is only 2%. This is attributed to the fact that it is difficult to prepare a corresponding concentrate at concentrations above 2%. At this time, the extracellular laccase activity of AnRcgL1 is 184.7 U/L, which is 2.1-fold higher than that before the addition of $MgSiO_3$ (Fig. 6C). However, the inhibitory effect of Al_2O_3 on AnRcgL1 extracellular laccase activity is independent of addition concentration (Fig. 6D).

The filamentous fungi mycelial morphology in liquid culture can be divided into three types, namely, mycelial pellets (including rough and smooth pellets), clumped aggregates, or dispersed mycelia [41]. To investigate the

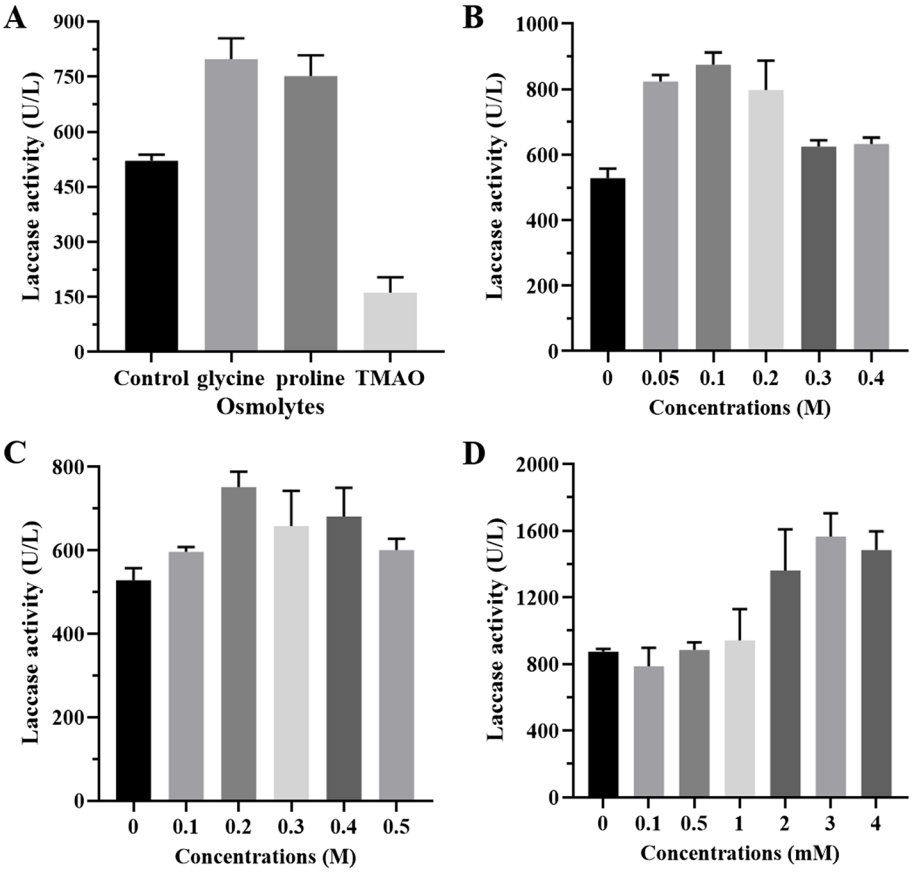

Fig. 7 Effect of osmolytes and Cu^{2+} on the extracellular Lcc9 production. **A** Effect of different osmolyte types. **B** Effect of varying the glycine concentration. **C** Effect of varying the proline concentration. **D** Effect of varying the Cu^{2+} concentration. Error bars represent the standard deviation

effect of microparticles on AnRcgL1 mycelial morphology, its morphological characteristics were observed under a microscope after shaking flask fermentation for 48 h. As shown in Fig. 6E, adding either $MgSiO_3$ or $CaCO_3$ significantly affected AnRcgL1 mycelial morphology except for Al_2O_3, transforming them from smooth pellets to rough pellets or freely dispersed mycelia.

Mycelial morphology influences the yield and productivity of target products from filamentous fungi by affecting heat, mass, and momentum transfer during submerged fermentation [31]. Filamentous fungi secrete proteins mainly at the mycelial tip, and when forming a mycelial pellet, it is more favorable for protein secretory expression in the surface thin layer than in the interior of the pellet [4]. In conclusion, the addition of $MgSiO_3$ or $CaCO_3$ in this study promoted the generation of mycelial morphology favorable for Lcc9 secretory expression during AnRcgL1 fermentation, which improved extracellular laccase activity.

Effect of osmolyte on Lcc9 production

To screen for osmolytes favorable for recombinant extracellular production of Lcc9, three osmolytes (0.2 M of TMAO, proline, and glycine) were added to the fermentation medium separately. As shown in Fig. 7A, the best osmolyte for Lcc9 production by AnRcgL1 was glycine, followed by proline, which increased extracellular laccase activity by 53% and 44%, respectively. However, adding TMAO reduced the extracellular laccase activity by 69% (Fig. 7A).

Since both glycine and proline can increase laccase activity and there is no significant difference ($p > 0.05$) between them, their optimal concentrations were further investigated separately. The results showed that the optimal concentrations of glycine and proline were 0.1 and 0.2 M, respectively. Under these conditions, the extracellular laccase activities of AnRcgL1 were 874.6 and 751.8 U/L (Fig. 7B and C), which were 1.7- and 1.4-fold higher than those without osmolytes, respectively.

Similarly, Dehghanpoor et al. found that adding 0.3 M glycine resulted in the highest recombinant peroxidase activity [42]. They suggested that altering the microenvironment of aromatic amino acids in the enzyme protein by adding osmolyte was responsible for increasing enzyme activity [42]. Furthermore, Norouzi et al. found that adding proline improves the stability of xylanase by inducing its conformational change [43]. Thus, these could also explain the increase in AnRcgL1 extracellular laccase activity after glycine and proline addition.

Effect of Cu^{2+} on Lcc9 production

By adding different concentrations (0.1, 0.5, 1, 2, 3 and 4 mM) of Cu^{2+} to the fermentation medium, it was found that the AnRcgL1 extracellular laccase activity first increased and then decreased with increasing Cu^{2+} concentration (Fig. 7D). When Cu^{2+} was added at a concentration of 3 mM, the AnRcgL1 extracellular laccase activity reached a maximum of 1566.7 U/L, which was 1.8-fold higher than that before addition (Fig. 7D).

Cu^{2+} can increase enzyme activity by increasing transcript levels of laccase-encoding genes and binding to their active sites during subsequent protein folding [44]. However, if the added Cu^{2+} concentration was too high, it inhibited mycelial growth and thus was unfavorable for laccase production [45]. This may be the reason why the AnRcgL1 extracellular laccase activity was reduced when the Cu^{2+} concentration exceeded 3 mM in this study (Fig. 7D).

Scale-up of Lcc9 production in a 1-L fermenter

To further verify the effect of gene expression cassette and bioprocess optimization on the extracellular Lcc9 production in *A. niger*, the recombinant strain AnRcgL1

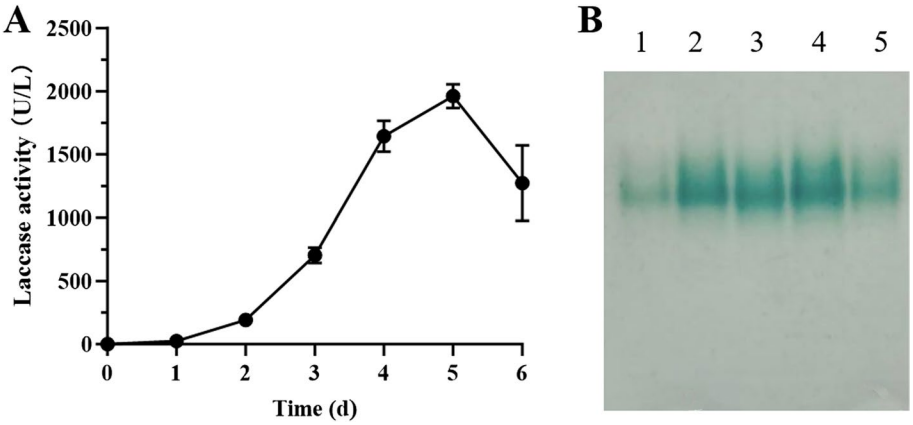

Fig. 8 Scale-up (1-L) fermentation of AnRcgL1. **A** The laccase activity in the fermentation supernatant was monitored as a function of time. Error bars represent the standard deviation. **B** Native-PAGE analysis of AnRcgL1 fermentation supernatant. Lanes 1–5: supernatant samples of AnRcgL1 at 2, 3, 4, 5, and 6 d, respectively

was fermented in a 1-L fermenter. As shown in Fig. 8A, the extracellular laccase activity of AnRcgL1 was 1961 U/L, which was 1.3-fold greater than that of its shake flask fermentation (1566.7 U/L). This result was validated by native-PAGE analysis (Fig. 8B). In conclusion, optimizing gene expression cassettes and recombinant strain bioprocesses is an effective strategy to enhance the recombinant extracellular expression of laccase Lcc9 in *A. niger*.

Conclusion

This study presents the first successful recombinant production of the *C. cinerea* laccase Lcc9 in *A. niger*. Recombinant Lcc9 production was improved by optimizing the gene expression cassette and bioprocess. The recombinant production level of Lcc9 was eventually increased from only a plate qualitative assay to an extracellular enzyme activity of 1566.7 and 1961 U/L in shake flasks and 1-L fermenter fermentations, respectively, with an increase of about 156.7-fold. In this process, *A. niger* transformation efficiency was increased 3.8-fold by optimizing the protoplast preparation system, and a novel efficient signal peptide, SP_{CAT}, was discovered that can be used in the *A. niger* expression system. Therefore, this study will not only advance the industrial production of Lcc9, but also improve the *A. niger* expression system.

Abbreviations

ABTS	2,2-Azino-bis (3-ethylbenzothiazoline-6-sulphonic acid)
CD	Czapex dox
Native-PAGE	Native-polyacrylamide gel electrophoresis
EDTA	Ethylene diamine tetraacetic acid
PDA	Potato dextrose agar
PEG	Polyethylene glycol
PMT	PEG-mediated transformation
qRT-PCR	Quantitative real-time PCR
SDS-PAGE	Sodium dodecyl sulfate–polyacrylamide gel electrophoresis
SP	Signal peptide
TMAO	Trimethylamine oxide
YPD	Yeast extract peptone dextrose

Supplementary Information

The online version contains supplementary material available at https://doi.org/10.1186/s12896-024-00924-8.

Additional file 1: Fig. S1. Fingerprinting of the protein with a molecular weight of approximately 95 kDa. (A) Mascot score histogram; (B) Protein search results. Fig. S2. Detection of *A. niger* mediated by different signal peptides on ABTS plates. Fig. S3. Native-PAGE results of AnGgcL fermentation supernatant. Lanes 1-5: supernatant samples of AnGgcL at 2, 3, 4, 5, and 6 d, respectively. Fig. S4. Detection of *A. niger* mediated by different promoters on ABTS plates. Fig. S5. Schematic structure of the plasmid pCCcg-*lcc9* (A) and pCRcg-*lcc9* (B). Fig. S6. Detection of *A. niger* obtained by different integration modes on ABTS plates. Table S1. Primers used in this study. Table S2. Signal peptides used in this study. Table S3. Promoters used in this study.

Additional file 2: Fig. S1. The original gel image of Fig. 4A. Fig. S2. The original gel image of Fig. 5A. Fig. S3. The original gel image of Fig. 8B. Fig. S4. The original gel image of Fig. S3A. Fig. S5. The original gel image of Fig. S3B.

Acknowledgements

We thank the support from Prof. Hua Zhang (School of Food and Biological Engineering, Hefei University of Technology) and associate Prof. Kangdi Hu (School of Food and Biological Engineering, Hefei University of Technology) for kindly providing the *A. niger* MA70.15 and plasmid pC3.

Authors' contributions

DBY designed the project, carried out experiments, and drafted the manuscript. XZL and HW carried out experiments. JJL revised the manuscript. ZMF and YZX supervised the project and revised the manuscript. All authors read and approved the final manuscript.

Funding

This work was supported by the Joint Funds of the National Natural Science Foundation of China (U22A20442), the National Key Research and Development Program (2021YFC2103000), the Key Projects for Scientific Research Projects of Higher Education Institutions in Anhui Province (2023AH050097), and the Doctoral Research Start-up Funding of Anhui University (S020318003/006).

Data availability

All data generated or analyzed during this study are included in this published article and its additional files.

Declarations

Ethics approval and consent to participate

Not applicable.

Consent for publication

Not applicable.

Competing interests

The authors declare no competing interests.

Author details

[1]School of Life Sciences, Anhui University, Hefei 230601, China. [2]Anhui Key Laboratory of Biocatalysis and Modern Biomanufacturing, Hefei 230601, China. [3]Anhui Provincial Engineering Technology Research Center of Microorganisms and Biocatalysis, Hefei 230601, China.

Received: 6 August 2024 Accepted: 15 November 2024
Published online: 22 November 2024

References

1. Barber-Zucker S, Mateljak I, Goldsmith M, Kupervaser M, Alcalde M, Fleishman SJ. Designed high-redox potential laccases exhibit high functional diversity. ACS Catal. 2022;12(21):13164–73.
2. Curran LMLK, Sale KL, Simmons BA. Review of advances in the development of laccases for the valorization of lignin to enable the production of lignocellulosic biofuels and bioproducts. Biotechnol Adv. 2022;54:107809.
3. Khatami SH, Vakili O, Movahedpour A, Ghesmati Z, Ghasemi H, Taheri-Anganeh M. Laccase: various types and applications. Biotechnol Appl Bioc. 2022;69(6):2658–72.
4. Li C, Zhou J, Du G, Chen J, Takahashi S, Liu S. Developing *Aspergillus niger* as a cell factory for food enzyme production. Biotechnol Adv. 2020;44:107630.
5. Liu D, Liu Q, Guo W, Liu Y, Wu M, Zhang Y, Li J, Sun W, Wang X, He Q. Development of genetic tools in glucoamylase-hyperproducing industrial *Aspergillus niger* strains. Biology. 2022;11(10):1396.
6. Zhang J, Liu C, Xie Y, Li N, Ning Z, Du N, Huang X, Zhong Y. Enhancing fructooligosaccharides production by genetic improvement of the industrial fungus *Aspergillus niger* ATCC 20611. J Biotechnol. 2017;249:25–33.
7. Li K, Zheng J, Yu L, Wang B, Pan L. Exploration of the strategy for improving the expression of heterologous sweet protein monellin in *Aspergillus niger*. J Fungi. 2023;9(5):528.
8. Dong L, Lin X, Yu D, Huang L, Wang B, Pan L. High-level expression of highly active and thermostable trehalase from *Myceliophthora*

thermophila in *Aspergillus niger* by using the CRISPR/Cas9 tool and its application in ethanol fermentation. J Ind Microbiol Biot. 2020;47(1):133–44.
9. Xu Y, Wang YH, Liu TQ, Zhang H, Zhang H, Li J. The GlaA signal peptide substantially increases the expression and secretion of alpha-galactosidase in *Aspergillus niger*. Biotechnol Lett. 2018;40(6):949–55.
10. Ali WB, Ayed AB, Turbe-Doan A, Bertrand E, Mathieu Y, Faulds CB, Lomascolo A, Sciara G, Record E, Mechichi T. Enzyme properties of a laccase obtained from the transcriptome of the marine-derived fungus *Stemphylium lucomagnoense*. Int J Mol Sci. 2020;21(21):8402.
11. Blumhoff M, Steiger MG, Marx H, Mattanovich D, Sauer M. Six novel constitutive promoters for metabolic engineering of *Aspergillus niger*. Appl Microbiol Biot. 2013;97(1):259–67.
12. Wang L, Xie Y, Chang J, Wang J, Liu H, Shi M, Zhong Y. A novel sucrose-inducible expression system and its application for production of biomass-degrading enzymes in *Aspergillus niger*. Biotechnol Biof Biop. 2023;16(1):23.
13. Schaepe P, Kwon MJ, Baumann B, Gutschmann B, Jung S, Lenz S, Nitsche B, Paege N, Schuetze T, Cairns TC, et al. Updating genome annotation for the microbial cell factory *Aspergillus niger* using gene co-expression networks. Nucleic Acids Res. 2019;47(2):559–69.
14. Chen X, Wang B, Pan L. Heterologous expression and characterization of *Penicillium citrinum* nuclease P1 in *Aspergillus niger* and its application in the production of nucleotides. Protein Expres Purif. 2019;156:36–43.
15. Wang S, Zhang P, Xue Y, Yan Q, Li X, Jiang Z. Characterization of a novel aspartic protease from *Rhizomucor miehei* expressed in *Aspergillus niger* and its application in production of ACE-inhibitory peptides. Foods. 2021;10(12):2949.
16. Iram A, Ozcan A, Yatmaz E, Turhan I, Demirci A. Effect of microparticles on fungal fermentation for fermentation-based product productions. Processes. 2022;10(12):2681.
17. Germec M, Karahalil E, Yatmaz E, Tari C, Turhan I. Effect of process parameters and microparticle addition on polygalacturonase activity and fungal morphology of *Aspergillus sojae*. Biomass Convers Bior. 2022;12(11):5329–44.
18. Rashid N, Thapliyal C, Chaudhuri P. Osmolyte induced enhancement of expression and solubility of human dihydrofolate reductase: an in vivo study. Int J Biol Macromol. 2017;103:1044–53.
19. Liu Y, Yu T, Zhang Y, Zhang H, Liu T, Li J. Secretory expression and properties of laccase from *Ganoderma lucidum* in *Aspergillus niger*. Sci Technol Food Ind. 2023;44(13):119–26. https://doi.org/10.13386/j.issn1002-0306.2022080103.
20. Ghany TMA, Bakri MM, Al-Rajhi AMH, Al Abboud MA, Alawlaqi MM, Shater ARM. Impact of copper and its nanoparticles on growth, ultrastructure, and laccase production of *Aspergillus niger* using corn cobs wastes. Bioresources. 2020;15(2):3289–306.
21. Feng H, Zhang D, Sun Y, Zhi Y, Mao L, Luo Y, Xu L, Wang L, Zhou P. Expression and characterization of a recombinant laccase with alkalistable and thermostable properties from *Streptomyces griseorubens* JSD-1. Appl Biochem Biotech. 2015;176:547–62.
22. Pan K, Zhao N, Yin Q, Zhang T, Xu X, Fang W, Hong Y, Fang Z, Xiao Y. Induction of a laccase Lcc9 from *Coprinopsis cinerea* by fungal coculture and its application on indigo dye decolorization. Bioresource Technol. 2014;162:45–52.
23. Guo S-X, Yao G-F, Ye H-R, Tang J, Huang Z-Q, Yang F, Li Y-H, Han Z, Hu L-Y, Zhang H. Functional characterization of a cystathionine β-synthase gene in sulfur metabolism and pathogenicity of *Aspergillus niger* in pear fruit. J Agric Food Chem. 2019;67(16):4435–43.
24. Liu J, Peng C, Han Q, Wang M, Zhou G, Ye B, Xiao Y, Fang Z, Kües U. *Coprinopsis cinerea* uses laccase Lcc9 as a defense strategy to eliminate oxidative stress during fungal-fungal interactions. Appl Environ Microb. 2022;88(1):e01760-01721.
25. Xu G, Wang J, Yin Q, Fang W, Xiao Y, Fang Z. Expression of a thermo-and alkali-philic fungal laccase in *Pichia pastoris* and its application. Protein Expres Purif. 2019;154:16–24.
26. Livak KJ, Schmittgen TD. Analysis of relative gene expression data using real-time quantitative PCR and the $2^{-\Delta\Delta CT}$ method. Methods. 2001;25(4):402–8.
27. Wikee S, Hatton J, Turbé-Doan A, Mathieu Y, Daou M, Lomascolo A, Kumar A, Lumyong S, Sciara G, Faulds CB. Characterization and dye decolorization potential of two laccases from the marine-derived fungus *Pestalotiopsis sp*. Int J Mol Sci. 2019;20(8):1864.
28. Yao D, Zhang K, Wu J. Available strategies for improved expression of recombinant proteins in *Brevibacillus* expression system: a review. Crit Rev Biotechnol. 2020;40(7):1044–58.
29. Qin L, Jiang X, Dong Z, Huang J, Chen X. Identification of two integration sites in favor of transgene expression in *Trichoderma reesei*. Biotechnol Biofuels. 2018;11:1–15.
30. Tokashiki J, Hayashi R, Yano S, Watanabe T, Yamada O, Toyama H, Mizutani O. Influence of alpha-1,3-glucan synthase gene *agsE* on protoplast formation for transformation of *Aspergillus luchuensis*. J Biosci Bioeng. 2019;128(2):129–34.
31. Gong Z, Zhang S, Liu J. Recent advances in chitin biosynthesis associated with the morphology and secondary metabolite synthesis of filamentous fungi in submerged fermentation. J Fungi. 2023;9(2):205.
32. Yao D, Su L, Li N, Wu J. Enhanced extracellular expression of *Bacillus stearothermophilus* α-amylase in *Bacillus subtilis* through signal peptide optimization, chaperone overexpression and α-amylase mutant selection. Microb Cell Fact. 2019;18:1–12.
33. Madhavan A, Pandey A, Sukumaran RK. Expression system for heterologous protein expression in the filamentous fungus *Aspergillus unguis*. Bioresource Technol. 2017;245:1334–42.
34. Madhavan A, Sukumaran RK. Signal peptides from filamentous fungi efficiently mediate the secretion of recombinant proteins in *Kluyveromyces lactis*. Biochem Eng J. 2015;102:31–7.
35. Zhu SY, Xu Y, Yu XW. Improved homologous expression of the acidic lipase from *Aspergillus niger*. J Microbiol Biotechnol. 2020;30(2):196–205.
36. Li H, Yao D, Pan Y, Chen X, Fang Z, Xiao Y. Enhanced extracellular raw starch-degrading α-amylase production in *Bacillus subtilis* by promoter engineering and translation initiation efficiency optimization. Microb Cell Fact. 2022;21(1):127.
37. Lu Y, Zheng X, Wang Y, Zhang L, Wang L, Lei Y, Zhang T, Zheng P, Sun J. Evaluation of *Aspergillus niger* six constitutive strong promoters by fluorescent-auxotrophic selection coupled with flow cytometry: a case for citric acid production. J Fungi. 2022;8(6):568.
38. Rao Y, Li P, Xie X, Li J, Liao Y, Ma X, Cai D, Chen S. Construction and characterization of a gradient strength promoter library for fine-tuned gene expression in *Bacillus licheniformis*. ACS Synth Biol. 2021;10(9):2331–9.
39. Li Y, Li C, Aqeel SM, Wang Y, Zhang Q, Ma J, Zhou J, Li J, Du G, Liu S. Enhanced expression of xylanase in *Aspergillus niger* enabling a two-step enzymatic pathway for extracting β-glucan from oat bran. Bioresource Technol. 2023;377:128962.
40. Gui Q, Deng S, Zhou Z, Cao W, Zhang X, Shi W, Cai X, Jiang W, Cui Z, Hu Z, et al. Transcriptome analysis in yeast reveals the externality of position effects. Mol Biol Evol. 2021;38(8):3294–307.
41. Cairns TC, Feurstein C, Zheng X, Zheng P, Sun J, Meyer V. A quantitative image analysis pipeline for the characterization of filamentous fungal morphologies as a tool to uncover targets for morphology engineering: a case study using *aplD* in *Aspergillus niger*. Biotechnol Biofuels. 2019;12:1–17.
42. Sarvandi-Dehghanpoor E, Riahi-Madvar A, Lotfi S, Torkzadeh-Mahani M. Improvement of kinetic properties and thermostability of recombinant *Lepidium draba* peroxidase (LDP) upon exposed to osmolytes. Int J Biol Macromol. 2018;119:1036–41.
43. Norouzi S, Birgani NH, Maghami P, Ariaeenejad S. Improvement of PersiXyn2 activity and stability in presence of trehalose and proline as a natural osmolyte. Int J Biol Macromol. 2020;163:348–57.
44. Fonseca MI, Ramos-Hryb AB, Fariña JI, Afanasiuk SSS, Villalba LL, Zapata PD. Effect of chemical and metallic compounds on biomass, mRNA levels and laccase activity of *Phlebia brevispora* BAFC 633. World J Microb Biot. 2014;30:2251–62.
45. Park J-W, Kang H-W, Ha B-S, Kim S-I, Kim S, Ro H-S. Strain-dependent response to Cu^{2+} in the expression of laccase in *Pycnoporus coccineus*. Arch Microbiol. 2015;197:589–96.

Publisher's Note